Article

Assessing the Impact of Light/Shallow Precipitation Retrievals from Satellite-Based Observations Using Surface Radar and Micro Rain Radar Observations

Chris Kidd [1,2,*] , **Edward Graham** [3] , **Tim Smyth** [4] and **Michael Gill** [5]

1   NASA/Goddard Space Flight Center, Greenbelt, MD 20771, USA
2   Earth System Science Interdisciplinary Center, University of Maryland, College Park, MD 20742, USA
3   Lews Castle College, University of the Highlands and Islands, Stornoway HS2 0XR, UK;
    Edward.Graham@uhi.ac.uk
4   Plymouth Marine Laboratory, Plymouth PL1 3DH, UK; tjsm@pml.ac.uk
5   Met Éireann Valentia Observatory, V23 Cahirciveen, Ireland; michael.gill@met.ie
*   Correspondence: chris.kidd@nasa.gov

Abstract: The accurate representation of precipitation across the Earth's surface is crucial to furthering our knowledge and understanding of the Earth System and its component processes. Precipitation poses a number of challenges, particularly due to the variability of precipitation over time and space and whether it falls as snow or rain. While conventional measures of precipitation are reasonably good at the location of their measurement, their distribution across the Earth's surface is uneven with some regions having no surface measurements. Spaceborne sensors have the capability of providing regular observations across the Earth's surface that can provide estimates of precipitation. However, the estimation of precipitation from satellite observations is not necessarily straightforward. Visible and/or infrared techniques rely upon imprecise cloud-top to surface precipitation relationships, while the sensitivity of passive microwave techniques to different precipitation types is not consistent. Active microwave (radar) observations provide the most direct satellite measurements of precipitation but cannot provide estimates close to the surface and are generally not sufficiently sensitive to resolve light precipitation. This is particularly problematic at mid to high latitudes, where light and/or shallow precipitation dominates. This paper compares measurements made by ground-based weather radars, Micro Rain Radars and the spaceborne Dual-frequency Precipitation Radar to study both light precipitation intensity and shallow precipitation occurrence and to assess their impact on satellites retrievals of precipitation at the mid to high latitudes.

Keywords: light precipitation; shallow precipitation; rainfall; snowfall; satellite precipitation estimation; micro rain radar

1. Introduction

The estimation of precipitation on a global scale is important for many applications. Knowing the distribution and quantity of precipitation is crucial to understanding and quantifying the global water and the associated energy cycle [1] and for better monitoring water resources that are fundamental to our economic and social wellbeing [2]. Crucially, at present there is a disparity between the observed and expected global precipitation totals [3], and despite its importance, the global measurement of precipitation is fraught with problems. Conventional measurements rely primarily upon rain or snow gauges which may be considered to be the most direct measure of precipitation at the surface. However, the accuracy of such measurements is limited by their ability to capture all the precipitation falling at the gauge location and for that location to faithfully represent the precipitation of the surrounding area [4,5]. Importantly, the distribution of these gauges across the Earth's surface is uneven with large areas having poor or no gauge coverage [6]. Weather radar systems provide frequent spatial measurements of precipitation, but the

coverage of such measurements is similar to that of the gauges, and imperfect radar backscatter to precipitation intensity relationships affect their overall accuracy [7]. Satellite-based sensors have the potential to provide truly global observations of precipitation, allowing estimates of precipitation to be made where few or no surface measurements are possible.

Observations made by satellite sensors provide a sample of the precipitation system at a particular point in time. Visible and infrared (IR) techniques observe the cloud tops and relate the cloud top characteristics (such as temperature, reflectivity and texture) to the precipitation at the Earth's surface [8]. Passive Microwave (PMW) observations respond to the hydrometeors along the atmospheric path between the Earth's surface and the satellite sensor, and although the observation is made instantaneously, the actual measurement is an integral of the hydrometeors through that atmospheric column [9]. The received radiation is a mix of an emission signal from liquid hydrometeors (particularly at the lower frequencies) and/or a scattering signal from frozen hydrometers (at higher frequencies). Active Microwave sensors (or radars), such as the Global Precipitation Measurement (GPM) mission [10,11], Dual-frequency Precipitation Radar (DPR) or the CloudSat Profiling Radar (CPR) [12] provide a vertical distribution of the hydrometeor concentrations, although they cannot retrieve precipitation close to the surface due to the clutter caused by backscatter from the surface. This also causes problems in determining the melting layer (where it exists) in the lowest levels [13]. For such radars, this usually relates to the lowest three to four range bins, or up to about 1000 m above the surface, although this increases towards the edge of swath (DPR) due to the inclined intersection of the footprint with the surface.

While quantitative satellite-based precipitation estimates have a long-established heritage [14], these products also have their drawbacks relating to the sensitivity of the observations to the precipitation at, or near, the surface. Many satellite products underestimate the precipitation with respect to surface observations, particularly at the mid to high latitudes [15–17], a result of the different forms and structures of the precipitation systems between the Tropics and higher latitudes. Behrangi and Yang [18] recently compared the GPM combined product [19] and surface gauge products [20] over the oceans and found large differences polewards of 40°N/S. Further studies using data from the CloudSat mission found that most satellite precipitation products significantly underestimate the occurrence of precipitation. Berg et al. [21] found that the Precipitation Radar (PR) on the Tropical Rainfall Measuring Mission (TRMM) only identified about 40% of the precipitation occurrences compared with CloudSat over the tropical ocean, while Suzuki et al. [22] highlighted the issue of the representation of light precipitation in models in their comparison of the observations from the Moderate Resolution Imaging Spectroradiometer (MODIS) and the CloudSat Profiling Radar (CPR). Using surface radar over the US, Lin and Hou [23] found that 43.1% of precipitation occurs at below 0.5 mm/h (the TRMM PR threshold), while 11.3% occurs at below 0.2 mm/h (the GPM DPR threshold). This underestimation is likely to be exacerbated, since spaceborne radar cannot observe close to the surface disproportionately affected higher latitudes where snowfall dominates [24,25], where shallow precipitation systems dominate [26] or where the precipitation falls as snow and is shallow [27]. Specific field campaigns, such as those organized through the GPM-GV [28], have provided a wealth of data to study such issues, although these are of limited extent, both spatially and temporally. Nevertheless, the retrieval of precipitation by spaceborne radars has been shown to be the most accurate [29], although often with a strong seasonal cycle imposed by the nature of the precipitation systems.

The underestimation of precipitation in satellite products can therefore be attributed to the sensitivity of the observations to light precipitation, the representation of snow (or mixed-phase) precipitation and the inability to retrieve near-surface/shallow precipitation or a combination of these. Since not all observing systems are affected to the same degree by each of these issues, the final products will be impacted differently. Moreover, deficiencies in these retrievals are often masked by their adjustment to better reflect the accumulations

from surface observations. Clearly, no single set of observations can adequately capture the full gamut of the characteristics of precipitation.

The purpose of this paper is therefore to better identify and quantify the contribution of light and/or shallow precipitation at the mid and high latitudes and the impact this has upon the spaceborne radar precipitation measurements. An initial analysis concentrates upon a comparison between the surface radar and satellite radar estimates to assess the contribute of light precipitation, followed by an analysis of data from two Micro Rain Radars (MRRs) to investigate the contribution of light precipitation in the vertical dimension.

2. Methodology

Three different radar datasets are used in this study to investigate the representation of the precipitation intensities and the vertical distribution of the precipitation from the surface upwards, particularly focusing upon light precipitation and the "blind zone" that the satellite precipitation radars encounter close to the surface. Surface based rainfall radar data are used to assess and quantify the large-scale contributions of light precipitation with those observed by the satellite-based observations, while measurements made by the MRRs are used to investigate the vertical distribution of precipitation and assess the impact upon the retrievals of precipitation from the GPM DPR, TRMM PR and CloudSat CPR close to the surface.

2.1. Data Sets

The three main datasets used in this analysis: surface weather radar, satellite-based DPR data and MRR observations.

2.1.1. Surface Weather Radar Data

Surface-based (weather) radars are now the mainstay of national and international precipitation measurements in many countries. They provide fine spatial and temporal scale measurements with good sensitivity to precipitation across all intensities. These radar measurements rely upon the backscatter of the radar signal by precipitation-size particles, although the properties of the backscatter-to-precipitation intensity varies, particularly between rainfall and snowfall. In addition, since the radar beams are elevated above the surface to avoid surface clutter, the altitude of the beam increases with increasing range from the radar (a 0.5-degree elevation results in the beam being approximately 2 km above the surface at a 200-km range). The precipitation products are usually available for a composite of radars that have been merged by the respective meteorological agencies and undergone quality control and calibration against rain gauge data to ensure consistency.

The surface radar data used in this paper is derived from the UK Met Office NIMROD product covering the United Kingdom and Ireland composited from 15 C-band rainfall radars and processed by the very short-range forecasting system [30]. The product is processed directly from the individual radar's polar (600 m × 1 degree) rain rate estimates to a 1 × 1 km grid with a temporal resolution of 5 min and quantitative resolution of 1/32 mm/h. The radar data undergoes basic quality control to account for the fundamental radar artefacts, quality control and calibration against the surface gauge data [31–33]. The 1 × 1 km data used here is also averaged over a 5 × 5 km area to better match the resolution (and precipitation characteristics) of the DPR. A total of 157,680 and 446,760 5-min surface radar samples were used for the PML and SSY locations, respectively.

2.1.2. DPR Radar

The DPR [34] on the GPM core satellite [11], launched in 2014, is the second spaceborne precipitation radar, following the TRMM PR. The DPR consists of Ku-band (13.6 GHz) and Ka-band (35.5 GHz) channels, which allow better estimates of rainfall and snowfall rates and, in particular, the particle size distributions and the phase (i.e., liquid or frozen) of the precipitation. The DPR provides precipitation estimates over both land and ocean across a swath of 245 km (Ku and Ka after 21 May 2018) and 125 km (Ka-only prior to 21 May 2018),

with an effective range resolution of 250 m. The 'near-surface' DPR measurements within 25 km of the principle MRR locations were extracted from the Level 2A V05 product (freely available from https://pmm.nasa.gov/data, accessed on 27 April 2021) and used at their native resolution of 5.4 × 5.4 km, with 31,425 and 47,564 samples available over the PML and SYY sites, respectively. The phase classification [33] was not used here, with the values deemed to be liquid water equivalent to match that of the MRR data. Note that, while the CPR has proved useful at identifying light precipitation, it has not been included in this study, since the nadir-only tracks of the sensor are not close to the MRR locations, and like the PR/DPR, the CPR too cannot retrieve shallow precipitation due to the limitation imposed by ground clutter.

2.1.3. MRR Data

MRRs are inexpensive ground-based vertically pointing radars [35]. Two main versions are currently available, the MRR-2 and MRR-Pro. The MRR-2 provides vertical measurements averaged over 1 min for 31 range bins, which can be set from 35 m through to 200 m, providing a total possible range of between 1085 m to 6200 m. The MRR-Pro provides 10 s measurements over 64, 128 or 256 of range bins, with the range bins set to between 10 m and 200 m. The radars operate at 24.1 GHz, with Doppler capability. By measuring the strength and the Doppler frequencies of the backscattered return signal, the fall velocities and size distribution of the droplets can be determined. Importantly, since the radar MRR is vertically pointing there is little surface clutter, although, typically, the very lowest range bins are usually avoided, and in this study, we used bins 2 (100–200 m) and above. Crucially, MRR observations are very sensitive to light precipitation and are available at fine resolution time scales.

Three mid-latitude coastal MRR sites were available for this study, located at the University of the Highland and Islands at Lewis Castle College in Stornoway (SYY), Scotland, at the Plymouth Marine Laboratory (PML) in Plymouth, UK and at Met Éireann, Valentia Observatory, Ireland (see Table 1). However, for the detailed analysis below, only the MRR-2 at the SYY site in NW Scotland and the PML MRR-Pro sited in SW England were used, since they currently provide multi-year observations. The SYY MRR provided more than 2M min of data from 15 June 2015 through 3 September 2019, while the PML MRR provided in excess of 800k min of data from 15 August 2019 to 22 February 2021, respectively.

Table 1. MRR locations used in this study.

Location	Abbreviation	Latitude	Longitude	Type
Stornoway (Scotland)	SYY	58°12′50.45″N	6°23′54.41″W	MRR-2
Plymouth (UK)	PML	50°21′57.60″N	4°08′57.71″W	MRR-Pro
Valentia (Ireland)	VAL	51°56′18.04″N	10°14′27.93″W	MRR-2

Figure 1 below shows a typical example of a precipitation system as measured by the MRR at Valentia in SW Ireland. Covering a 24-h period from noon 31 August to noon 1 September 2020, this example shows a period of moderate precipitation, as shown by the higher precipitation intensities and faster fall velocities. After this, the precipitation is generally much lighter (<1 mm/h) and below 1 km in altitude. Clearly, while the spaceborne precipitation radars are likely to be able to detect the initial period of the precipitation, the later portion of the precipitation system would be more challenging.
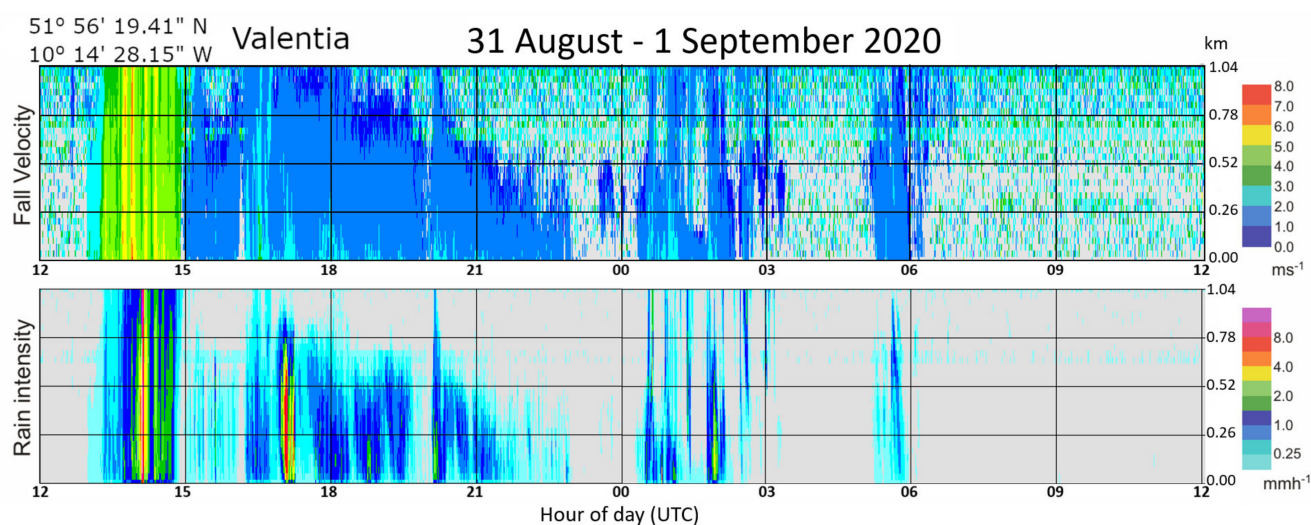
Figure 1. Retrieval of the fall velocity and rain intensity during a precipitation event over the Valentia (SW Ireland) MRR site for 31 August through 1 September 2020. Note the vertical scale, from 0 to 1.04 km, showing that much of the precipitation was below 1 km, with a dominance of light rain intensities of 1 mm/h or less.

2.2. Data Processing

Processing of the different data sets aims to provide, where possible, near coincident data to ensure that similar precipitation systems were being observed and measured. The surface radar data, available at 1-km 5-min resolution, was also subsampled to 5-km resolution to a similar resolution to that of the DPR and, thus, provided 1-km and 5-km resolution measurements of (near) surface precipitation. The SYY MRR was located ca.13 km from the UK Met Office C-band radar at Druim a Starraig near Stornoway on the Isle of Lewis, Scotland, while the PML MRR is located about 87 km and 83 km from the Predannack and the Cobbacombe Cross radars in England, respectively. Assuming a 0.5-degree beam elevation, this equates to the beam being approximately 0.12, 0.76 and 0.72 km above the surface for each of the three radar sites, respectively. The data from the PML MRR-Pro was available at 25- and 35-m range gate resolution every 10 s: this data was averaged into 100-m bins over 60 s to better match the range and temporal sampling of the SYY MRR-2. The data from the DPR instrument was extracted for an area 25 km around each of the MRR locations to ensure sufficient observations were available to make useful comparisons due to the limited sampling of the DPR as a result of the orbital characteristics.

3. Results

3.1. Occurrence of Precipitation

The occurrence of precipitation was analyzed using a cumulative distribution plot, as shown in Figure 2. Here, the cumulative log distributions of the intensities were presented for the MRR, DPR and the surface radar at 1-km and 5-km resolutions for both the PML (continuous line) and SYY (dashed line) locations. The poor sensitivity of the DPR to light precipitation is clearly shown, with the instrument identifying virtually no precipitation below about 0.2 mm/h. This contrast with an occurrence of 30% for the 1-km surface radar data and between 40% and 50% for the 5-km surface radar and MRR measurements. Given that the 5-km resolution product from the surface radar is close to that of the DPR footprints (5.4 × 5.4 km), it is clear that the sensitivity of the DPR is crucial, since it only identified about half of the precipitation of the surface radar. Even at 0.5 mm/h, the DPR identified 25–30% of the precipitation compared with 55–72% of that identified by the surface radar and MRR measurements.
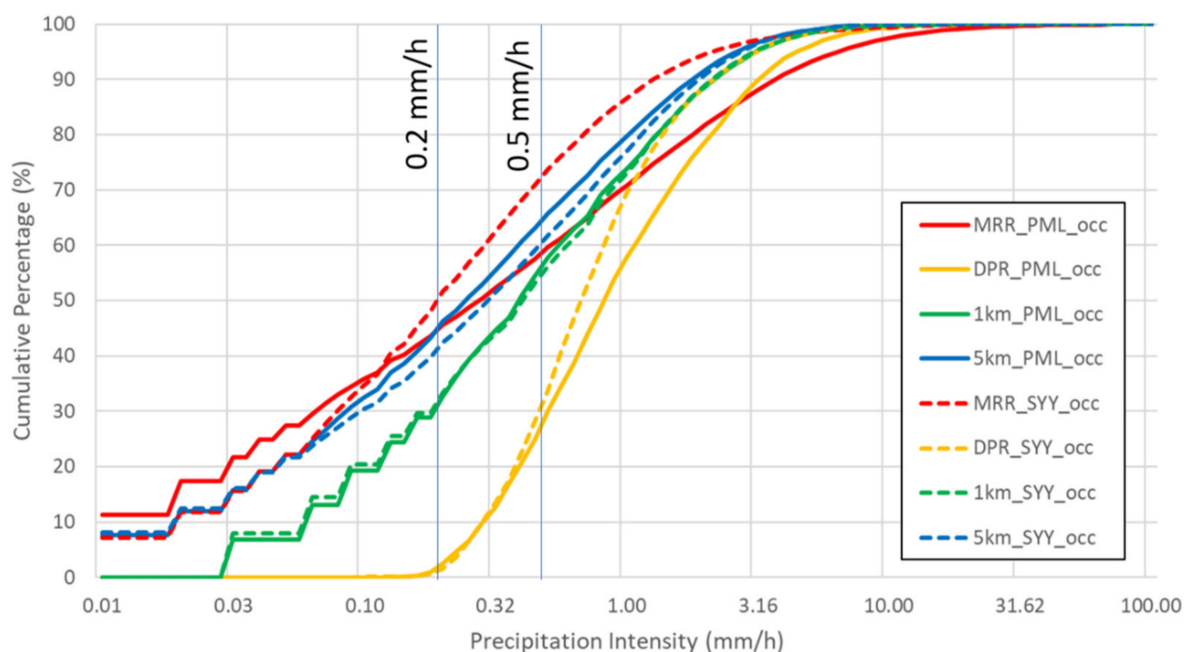
Figure 2. Occurrence of precipitation as observed at the PML (continuous lines) and SYY (dashed lines) locations for the MRR (red), DPR (yellow), 1-km radar (green) and 5-km radar (blue).

Considering the measurements made by the individual instruments, the 1-km surface radar distributions are virtually identical between the PML and SYY sites, suggesting only small differences between their precipitation regimes at this scale. While, at 5-km, there are small differences between the two sites, these are minor and, when combined with the 1-km resolution data, might suggest subtle differences in the spatial extent of the precipitation systems between the two sites. The light rain rate differences between the DPR measurements at PML and SYY are negligible, although the differences increase with the increasing intensity. The MRR measurements differ between the two sites at intensities at or above about 1 mm/h. It should be noted that the greater occurrence of moderate-to-heavy precipitation seen by the PML MRR is likely to be due to a combination of the point measurements of the MRR and precipitation characteristics. Although quite large differences are apparent between the MRR and DPR distributions, at least these are consistent between the SYY and PML distributions.

3.2. Accumulation of Precipitation

The accumulation cumulative distribution curves shown in Figure 3 show the cumulative proportion of the precipitation that contributes to the total precipitation. Here, all the distributions, except the MRR measurements, are reasonably similar, although the DPR tends to be on the low side at light intensities. At 0.2 mm/h, the precipitation contribution to the DPR total precipitation is essentially zero, while at 0.5 mm/h, the DPR accumulation is between 5% (at PML) and 10% (at SYY). The light rain contribution measured by the surface radar, for comparison, is between 10% and 15% for the 1- and 5-km resolutions. The significant divergence of the MRR distribution at the higher precipitation intensities is, however, evident. This is likely to be due to the at-surface point-resolution of the MRR data being more likely to measure high intensity events than the area-averaged 1-km or 5-km footprints of the surface radar and DPR data. The differences between the 1-km and 5-km resolution radar products are small, since they are generated from the same dataset, and therefore, the total precipitation should be the same, regardless of the resolution.
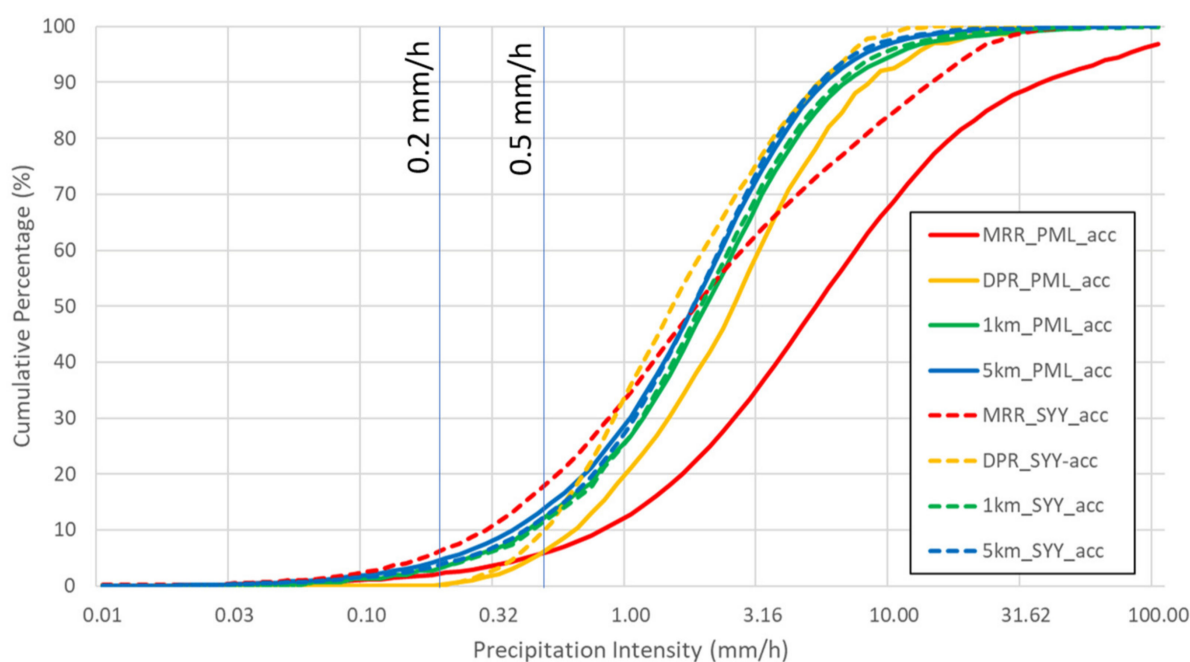
Figure 3. Accumulation of precipitation as observed at the PML (continuous lines) and SYY (dashed lines) locations for the MRR (red), DPR (yellow), 1-km radar (green) and 5-km radar (blue).

3.3. Impact of Spatial Resolution Using Surface Radar

Although the resolution is a key factor in determining the identification of precipitation within a radar or satellite sampling area (i.e., footprint), the scale relationship is not straightforward, not least since it depends upon the spatial heterogeneity of the precipitation system being observed. While, in Figures 2 and 3, the surface radar observations at 1 km and 5 km were similar, if the two different resolutions are compared substantial differences can be seen. This is particularly noticeable for the cumulative occurrence and accumulation of precipitation at different rain/no-rain thresholds, as shown in Figure 4.

Considering the occurrence of precipitation first, it can be seen from Figure 4a–c that at the 0.2-mm/h threshold differences between the 1-km radar and 5-km radar resolutions are relatively small, with the trend lines close to the 1:1 line. However, at the SYY location, a good number of the monthly values are below the 1:1 line, suggesting more variability than that experienced at the PML site. Increasing the threshold to 0.5 mm/h results in a greater separation of the 1-km to 5-km relationship of the PML and SYY locations, while at 1 mm/h, the SYY 1-km resolution occurrence is markedly greater than the 5-km resolution occurrence, a consequence of the 'beam-filling' effect over a larger footprint. It can be seen that the 1-km to 5-km relationship over the PML location is fairly consistent, with the 5-km occurrence being slightly higher than that of the 1-km observations.

In terms of accumulation (Figure 4d–f), the contribution of light precipitation below the different thresholds shows a different distribution to that shown by the occurrence of precipitation. At the 0.2-mm/h threshold, there is some divergence in between the PML and SYY trends, which increases at the 0.5- and 1.0-mm/h thresholds. At the 1.0-mm/h threshold, there is a clear difference in the relationship between the contributions made to the accumulation for the SYY and PML sites. While differences are possible between the two MRR systems, these have been calibration, and past intercomparisons have shown a good degree of consistency in their measurements. Another possible explanation is that the size of precipitation systems seen over the PML location are larger. Conversely, over the SYY site, such systems are smaller and of light precipitation, such that when averaged over a 5 × 5-km area, they do not meet the higher rain/no-rain threshold.
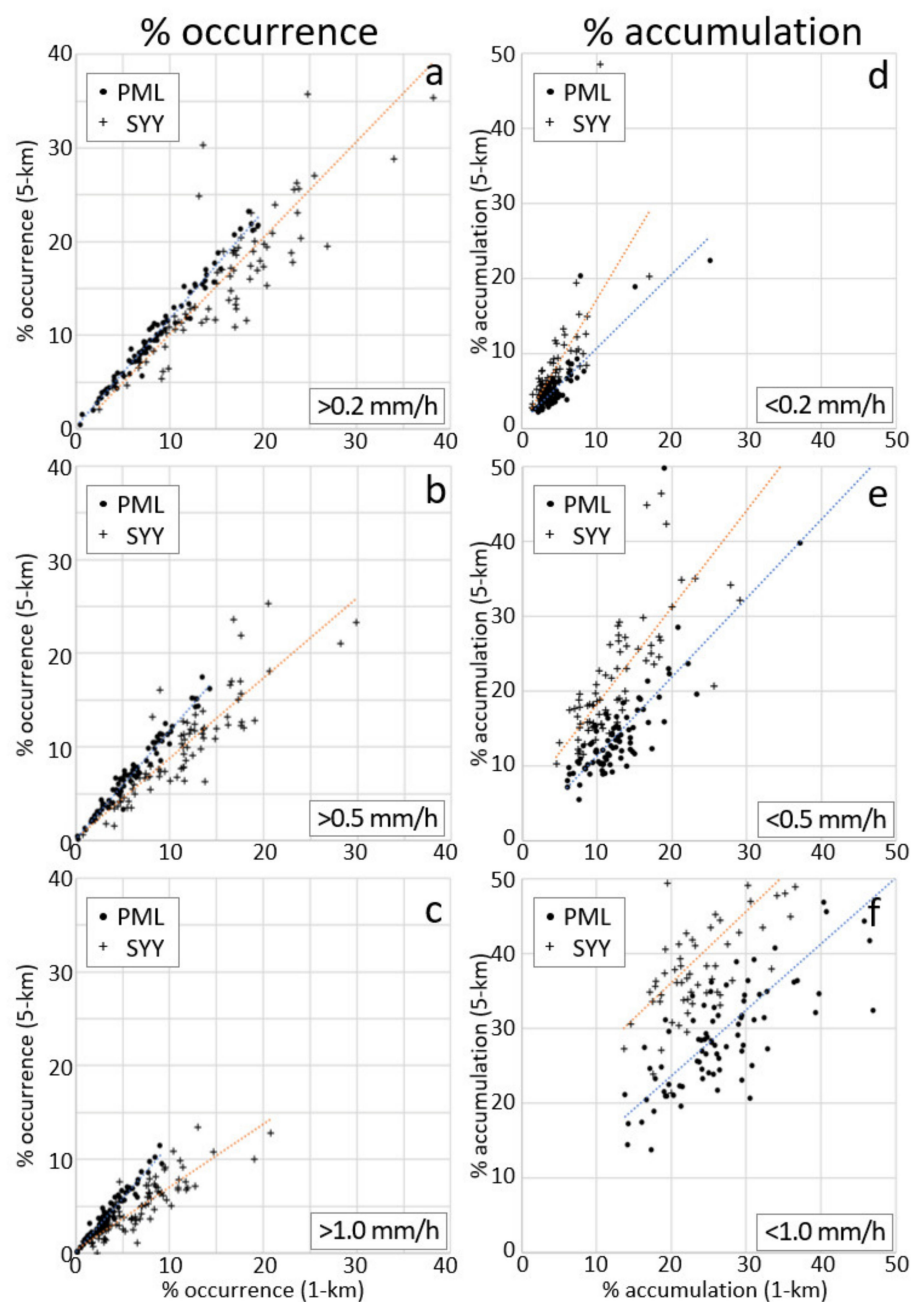
Figure 4. Comparison of the 1-km and 5-km surface radar resolution datasets showing the % occurrence of precipitation (**a–c**) above and proportion of the accumulation (**d–f**) below the thresholds set at 0.2, 0.5 and 1.0 mm/h. Dots represent the data for Plymouth (PML) and the crosses for Stornoway (SYY), while the dotted lines present the linear trend lines of each dataset. Each point represents the occurrence or accumulation calculated for each month from 2014 to 2020.

3.4. Representation of Light Precipitation with Height

While the occurrence and accumulation are important for understanding the characteristics of the precipitation of the different sites being studied, the characteristics of the precipitation with height are crucial to understand what the spaceborne precipitation radars should observe and retrieve. Consequently, the MRR datasets were processed to extract the occurrence of precipitation at different rain rate threshold at different heights to simulate the retrieval capabilities of the DPR. The results are presented in Table 2 below.

Table 2. Occurrence of precipitation by profile for SYY and PML. (Note the 'at-surface' precipitation is deemed to be precipitation in range bin 2 covering the 100–200-m altitude).

	SYY 16-05-2015:03-09-2019			PML 15-08-2019:22-02-2021		
	Number of Profiles	% of All Profiles	% of Raining Profiles	Number of Profiles	% of All Profiles	% of Raining Profiles
Number of all valid profiles	2,132,508	100.0%		748,179	100.0%	
Profiles with > 0.0	342,385	16.1%	100.0%	117,818	15.7%	100.0%
Profiles with ≥0.2	264,014	12.4%	77.1%	87,107	11.6%	73.9%
Profiles with ≥ 0.5	209,544	9.8%	61.2%	73,777	9.9%	62.6%
Profiles with > 0.0 above 1000 m	276,400	13.0%	80.7%	92,722	12.4%	78.7%
Profiles with ≥ 0.2 above 1000 m	218,874	10.3%	63.9%	72,657	9.7%	61.7%
Profiles with ≥ 0.5 above 1000 m	176,572	8.3%	51.6%	62,600	8.4%	53.1%
Profiles with > 0.0 above 1500 m	220,513	10.3%	64.4%	76,267	10.2%	64.7%
Profiles with ≥ 0.2 above 1500 m	173,054	8.1%	50.5%	61,784	8.3%	52.4%
Profiles with ≥ 0.5 above 1500 m	138,985	6.5%	40.6%	53,267	7.1%	45.2%

In terms of sensitivity to precipitation (>0.0 mm/h), the two sites are similar with 16.1% of all profiles at SYY having precipitation at the surface, compared with 15.7% of PML profiles. Of these raining profiles, above the 0.2-mm/h threshold, SYY (PML) has 77.1% (73.8%), and above 0.5 mm/h, SYY (PML) has 61.2% (62.6%). Taking the lowest altitude that the DPR can provide clutter-free data [36], the occurrence of the precipitation fell to 80% (SYY) and 78.7% (PML) at 1000 m or 64% and 64.7% at 1500 m, respectively. Crucially, when the height and sensitivity (the no-rain/rain threshold) were combined, these values fell to 63.9% (SYY) and 61.7% (PML) at 1000 m and 0.2 mm/h and 51.6% and 53.1% at 1000 m and 0.5 mm/h, respectively. Given the minimum detectable precipitation and lowest altitude retrieval, this implies that the DPR is only capable of identifying and retrieving about 50% of the precipitation that occurs at these mid-latitude locations. It should be noted, however, that the MRR measurements are made at a point location. Nevertheless, as shown in Figure 2, at the DPR resolution there appears to have relatively small differences in the identification of precipitation between the 5-km (DPR resolution) surface radar and MRR.

4. Discussion

The results shown above indicate that the representation of the occurrence of light precipitation is impacted by the rain/no-rain sensitivity of the observing system, although less so in terms of the accumulation of the 'at-surface' precipitation. However, analyzing the MRR data, the impact of the occurrence of shallow precipitation is significant when accounting for the sensitivity at the height at which the satellite precipitation radars are able to provide their retrievals. Although there are issues with scale mismatches necessitating caution when interpreting the results, they show that the observation of precipitation occurrence across different scales is fairly robust and probably more so than that of precipitation accumulation.

The initial results show that light and shallow precipitation are under-represented by the current satellite-based precipitation radar observations. The impact of this becomes increasingly significant at the mid and high latitudes, where the light and shallow precipitation systems dominate. Further studies are needed to better quantify the magnitude of

this, both regionally and temporally. Crucially, knowing how much precipitation is not being observed is important in improving the retrieval schemes for precipitation both over these regions and globally. In addition, it is also important any corrections are correctly applied to avoid introducing poorly constructed adjustments.

While the numbers shown above are summaries of aggregated data, the users should bear in mind the observational capability of the instruments in relationship to what is being measured. Like Figure 1 above, Figure 5 shows an example of the MRR data from the PML site for 29–30 January 2021. During the initial period of precipitation, the DPR should have no problem in identifying and retrieving precipitation, since there is moderate-to-heavy liquid precipitation at and above 1.4 km, well within the capabilities of the DPR instrument. Later on, however, after 0900UTC on 30 January, the freezing/melting level dropped to about 1.4 km. While the DPR might be able to see this precipitation at nadir, towards the edge of its swath, the liquid precipitation may not be within the 1500-m minimum detectable height, with only frozen hydrometeors providing any backscatter signal. After about 1300UTC, although the precipitation intensity remains between about 2–4 mm/h, the depth of the precipitation is largely below 1.4 km, while after 1400UTC, the precipitation is very light <0.5 mm/h and below about 800 m. It is clear, therefore, that the DPR will see some, but not necessarily all, of the precipitation.
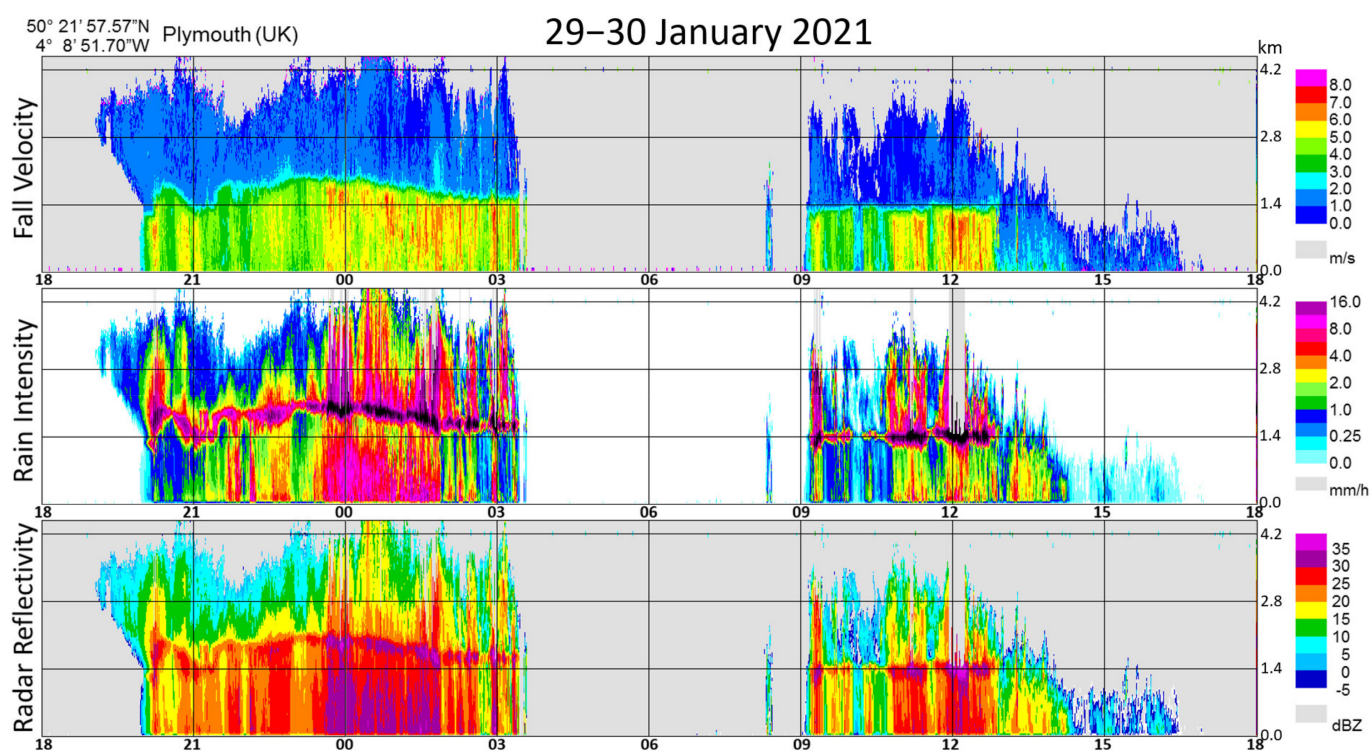

Figure 5. Example of a plot of data for 18:00 UTC on 29 January 2021 through to 18:00 UTC on 30 January 2021. The top plot shows the fall velocity, the middle plot the rain intensity and the bottom plot the radar reflectivity. The temporal sampling is 10 s, with 128 range bins with a range resolution of 35 m. The height of the melting layer is easily discernible by the change in the fall velocities and high rain rates and reflectivities about 1.4 km above the surface.

5. Conclusions

This paper presented a comparison and assessment of the precipitation characteristics over a mid-latitude region. Data from both satellite estimates and ground-based measurements have been compared, showing that the satellite estimates underestimate the true precipitation occurrence and accumulation. Based upon the measurements from the surface-based MRR data, these can be summarized as:

(i)   Spaceborne radar systems are limited by the current technology and trade-offs between resolution, power and sensitivity [37]. The TRMM PR had a rain/no-rain sensitivity of about 0.5 mm/h, while the GPM DPR, more relevant for mid-latitude studies, had a nominal rain/no-rain sensitivity of about 0.5 mm/h for the Ku-only or 0.2 mm/h for the combined Ka/Ku retrievals. The impact of sensitivity alone means that the DPR would only see about 75% of the precipitation occurrence for the Ka/Ku retrievals, falling to about 62% for the Ku retrieval alone.

(ii)   At-surface retrievals from spaceborne radars are limited by the surface return or clutter. In the case of the PR and DPR, this is about 1000 m at nadir, increasing to about 1500 m at the edge of the radar swath or higher in regions with high relief or varied terrain. If rainfall as identified by the MRR at the surface is considered, typically, only in 80% of the cases is there precipitation at or above 1000 m or 64% at or above 1500 m.

(iii)   Combining the effects of sensitivity and height, if both the sensitivity and height criteria are analyzed, then in only about 62% to 63% of cases, where precipitation is seen at the surface, is precipitation present above 1000 m at intensities at or above 0.2 mm/h, falling to about 52% to 53% at or above 0.5 mm/h.

The implications of these findings are that, at mid to high latitudes, the spaceborne radar may not be able to observe about half of all precipitation occurrences. Furthermore, since retrieval schemes such as the Goddard Profiling scheme (GPROF) and products such as the GMI-DPR combined rely upon the DPR information ultimately for their retrievals, if the DPR does not see precipitation, neither do they. The GPROF scheme has attempted to rectify this by incorporating surface radar (from over the US), but the implementation of this is limited to cold surface types and not more generally across the mid and high latitudes.

Crucially, it is vital that the spatial and temporal scales of the observations are clearly identified, since these often dictate the characteristics of precipitation, such as the occurrence. This is a multi-faceted problem, since, while the occurrence of precipitation will increase with larger footprints, the mean rain rate will decrease; thus, a larger footprint will require greater sensitivity to identify the precipitation. For example, the CloudSat CPR has a 1.4×1.7-km footprint compared to the GPM DPR with 5.4×5.4 km: the DPR should see a higher occurrence of precipitation, but a lower sensitivity (Ku 15 dBZ and Ka 14–19 dBZ vs. CPR < -29 dBZ) means that it is less likely to capture the light precipitation.

The results of this paper exemplify the complexities when trying to relate satellite observations to the characteristics of the precipitation at the surface. Ultimately, to better understand these precipitation characteristics, it is necessary that the spatial and temporal resolutions of the observations are commensurate with those of the precipitation.

References

1. L'Ecuyer, T.S.; Beaudoing, H.K.; Rodell, M.; Olson, W.; Lin, B.; Kato, S.; Clayson, C.A.; Wood, E.; Sheffield, J.; Adler, R.; et al. The Observed State of the Energy Budget in the Early Twenty-First Century. *J. Clim.* **2015**, *28*, 8319–8346. [CrossRef]
2. Kirschbaum, D.B.; Huffman, G.J.; Adler, R.F.; Braun, S.; Garrett, K.; Jones, E.; McNally, A.; Skofronick-Jackson, G.; Stocker, E.; Wu, H.; et al. NASA's Remotely Sensed Precipitation: A Reservoir for Applications Users. *Bull. Am. Meteorol. Soc.* **2017**, *98*, 1169–1184. [CrossRef]
3. Trenberth, K.E.; Fasullo, J.T.; Kiehl, J. Earth's Global Energy Budget. *Bull. Am. Meteorol. Soc.* **2009**, *90*, 311–324. [CrossRef]
4. Sevruk, B. Regional dependency of precipitation-altitude relationship in the swiss ALPS. *Clim. Chang.* **1997**, *36*, 355–369. [CrossRef]
5. Dorninger, M.; Schneider, S.; Steinacker, R. On the interpolation of precipitation data over complex terrain. *Theor. Appl. Clim.* **2008**, *101*, 175–189. [CrossRef]
6. Kidd, C.; Becker, A.; Huffman, G.J.; Muller, C.L.; Joe, P.; Skofronick-Jackson, G.; Kirschbaum, D.B. So, How Much of the Earth's Surface Is Covered by Rain Gauges? *Bull. Am. Meteorol. Soc.* **2017**, *98*, 69–78. [CrossRef]
7. Illingworth, A.J.; Blackman, T.M. The Need to Represent Raindrop Size Spectra as Normalized Gamma Distributions for the Interpretation of Polarization Radar Observations. *J. Appl. Meteorol.* **2002**, *41*, 286–297. [CrossRef]
8. Hong, Y.; Hsu, K.-L.; Sorooshian, S.; Gao, X. Precipitation Estimation from Remotely Sensed Imagery Using an Artificial Neural Network Cloud Classification System. *J. Appl. Meteorol.* **2004**, *43*, 1834–1853. [CrossRef]
9. Kummerow, C.D. Introduction to Passive Microwave Retrieval Methods. In *Advances in Global Change Research*; Levizzani, V., Kidd, C., Kirschbaum, D.B., Kummerow, C.D., Nakamura, K., Turk, F.J., Eds.; Springer Nature: Cham, Switzerland, 2020; Volume 67, pp. 123–140.
10. Hou, A.Y.; Kakar, R.K.; Neeck, S.; Azarbarzin, A.A.; Kummerow, C.D.; Kojima, M.; Oki, R.; Nakamura, K.; Iguchi, T. The global precipitation measurement mission. *Bull. Am. Meteorol. Soc.* **2014**, *95*, 701–722. [CrossRef]
11. Skofronick-Jackson, G.; Petersen, W.A.; Berg, W.; Kidd, C.; Stocker, E.F.; Kirschbaum, D.B.; Kakar, R.; Braun, S.A.; Huffman, G.J.; Iguchi, T.; et al. The Global Precipitation Measurement (GPM) Mission for Science and Society. *Bull. Am. Meteorol. Soc.* **2017**, *98*, 1679–1695. [CrossRef]
12. Stephens, G.L.; Vane, D.G.; Tanelli, S.; Im, E.; Durden, S.; Rokey, M.; Reinke, D.; Partain, P.; Mace, G.G.; Austin, R.; et al. CloudSat mission: Performance and early science after the first year of operation. *J. Geophys. Res. Space Phys.* **2008**, *113*, 18. [CrossRef]
13. Kidd, C.; Levizzani, V. Status of satellite precipitation retrievals. *Hydrol. Earth Syst. Sci.* **2011**, *15*, 1109–1116. [CrossRef]
14. Watters, D.; Battaglia, A.; Mroz, K.; Tridon, F. Validation of the GPM Version-5 Surface Rainfall Products over Great Britain and Ireland. *J. Hydrometeorol.* **2018**, *19*, 1617–1636. [CrossRef]
15. Barrett, E.C.; Dodge, J.; Goodman, H.M.; Janowiak, J.; Kidd, C.; Smith, E.A. The first WetNet precipitation intercomparison project (PIP-1). *Remote Sens. Rev.* **1994**, *11*, 49–60. [CrossRef]
16. Barrett, E.C.; Adler, R.F.; Arpe, K.; Bauer, P.; Berg, W.; Chang, A.; Ferraro, R.; Ferriday, J.; Goodman, S.; Hong, Y.; et al. The first WetNet Precipitation Inter-comparison Project: Interpretation of Results. *Remote Sens. Rev.* **1994**, *11*, 303–373. [CrossRef]
17. Adler, R.F.; Kidd, C.; Petty, G.W.; Morissey, M.; Goodman, H.M. Intercomparison of Global Precipitation Products: The Third Precipitation Intercomparison Project (PIP–3). *Bull. Am. Meteorol. Soc.* **2001**, *82*, 1377–1396. [CrossRef]
18. Behrangi, A.; Yang, S. A new estimate for oceanic precipitation amount and distribution using complementary precipitation observations from space and comparison with GPCP. *Environ. Res. Lett.* **2020**, *15*, 124042. [CrossRef]
19. Grecu, M.; Olson, W.S. *Precipitation Retrievals from Satellite Combined Radar and Radiometer Observations*; Levizzani, V., Kidd, C., Kirschbaum, D.B., Kummerow, C.D., Nakamura, K., Turk, F.J., Eds.; Springer Nature: Cham, Switzerland, 2020; Volume 67, pp. 231–248.
20. Becker, A.; Finger, P.; Meyer-Christoffer, A.; Rudolf, B.; Schamm, K.; Schneider, U.; Ziese, M. A description of the global land-surface precipitation data products of the Global Precipitation Climatology Centre with sample applications including centennial (trend) analysis from 1901–present. *Earth Syst. Sci. Data* **2013**, *5*, 71–99. [CrossRef]
21. Berg, W.; L'Ecuyer, T.; Haynes, J.M. The Distribution of Rainfall over Oceans from Spaceborne Radars. *J. Appl. Meteorol. Clim.* **2010**, *49*, 535–543. [CrossRef]
22. Suzuki, K.; Stephens, G.L.; Heever, S.C.V.D.; Nakajima, T.Y. Diagnosis of the Warm Rain Process in Cloud-Resolving Models Using Joint CloudSat and MODIS Observations. *J. Atmos. Sci.* **2011**, *68*, 2655–2670. [CrossRef]
23. Lin, X.; Hou, A.Y. Estimation of Rain Intensity Spectra over the Continental United States Using Ground Radar–Gauge Measurements. *J. Clim.* **2012**, *25*, 1901–1915. [CrossRef]
24. Kulie, M.S.; Bennartz, R. Utilizing Spaceborne Radars to Retrieve Dry Snowfall. *J. Appl. Meteorol. Clim.* **2009**, *48*, 2564–2580. [CrossRef]
25. Behrangi, A.; Christensen, M.; Richardson, M.; Lebsock, M.; Stephens, G.; Huffman, G.J.; Bolvin, D.; Adler, R.F.; Gardner, A.; Lambrigtsen, B.; et al. Status of high-latitude precipitation estimates from observations and reanalyses. *J. Geophys. Res. Atmos.* **2016**, *121*, 4468–4486. [CrossRef]
26. Short, D.A.; Nakamura, K. TRMM radar observations of shallow precipitation over the tropical oceans. *J. Clim.* **2000**, *13*, 4107–4124. [CrossRef]
27. Kulie, M.S.; Milani, L.; Wood, N.B.; Tushaus, S.A.; Bennartz, R.; L'Ecuyer, T.S. A Shallow Cumuliform Snowfall Census Using Spaceborne Radar. *J. Hydrometeorol.* **2016**, *17*, 1261–1279. [CrossRef]

28. Petersen, W.A.; Kirstetter, P.-E.; Wang, J.; Wolff, D.B.; Tokay, A. *The GPM Ground Validation Program*; Levizzani, V., Kidd, C., Kirschbaum, D.B., Kummerow, C.D., Nakamura, K., Turk, F.J., Eds.; Springer Nature: Cham, Switzerland, 2020; Volume 69, pp. 471–502.

29. Kidd, C.; Tan, J.; Kirstetter, P.; Petersen, W.A. Validation of the Version 05 Level 2 precipitation products from the GPM Core Observatory and constellation satellite sensors. *Q. J. R. Meteorol. Soc.* **2018**, *144*, 313–328. [CrossRef]

30. Met Office. 1 km Resolution UK Composite Rainfall Data from the Met Office Nimrod System. NCAS British Atmospheric Data Centre. 2003. Available online: https://catalogue.ceda.ac.uk/uuid/27dd6ffba67f667a18c62de5c3456350 (accessed on 3 March 2021).

31. Harrison, D.L.; Scovell, R.W.; Kitchen, M. High-resolution precipitation estimates for hydrological uses. *Proc. Inst. Civ. Eng. Water Manag.* **2009**, *162*, 125–135. [CrossRef]

32. Harrison, D.L.; Norman, K.; Pierce, C.; Gaussiat, N. Radar products for hydrological applications in the UK. *Proc. Inst. Civ. Eng. Water Manag.* **2012**, *165*, 89–103. [CrossRef]

33. Fairman, J.G.; Schultz, D.M.; Kirshbaum, D.J.; Gray, S.L.; Barrett, A.I. A radar-based rainfall climatology of Great Britain and Ireland. *Weather* **2015**, *70*, 153–158. [CrossRef]

34. Iguchi, T. Dual-Frequency Precipitation Radar (DPR) on the Global Precipitation Measurement (GPM) Mission's Core Observatory. In *Advances in Global Change Research*; Levizzani, V., Kidd, C., Kirschbaum, D.B., Kummerow, C.D., Nakamura, K., Turk, F.J., Eds.; Springer Nature: Cham, Switzerland, 2020; Volume 67, pp. 183–192.

35. Peters, G.; Fischer, B.; Andersson, T. Rain observations with a vertically looking Micro Rain Radar (MRR). *Boreal Environ. Res.* **2002**, *7*, 353–362.

36. Skofronick-Jackson, G.; Kulie, M.; Milani, L.; Munchak, S.J.; Wood, N.B.; Levizzani, V. Satellite Estimation of Falling Snow: A Global Precipitation Measurement (GPM) Core Observatory Perspective. *J. Appl. Meteorol. Clim.* **2019**, *58*, 1429–1448. [CrossRef] [PubMed]

37. Battaglia, A.; Kollias, P.; Dhillon, R.; Lamer, K.; Khairoutdinov, M.; Watters, D. Mind the gap—Part 2: Improving quantitative estimates of cloud and rain water path in oceanic warm rain using spaceborne radars. *Atmos. Meas. Tech.* **2020**, *13*, 4865–4883. [CrossRef]